n-p bremsstrahlung interpretation of high energy gamma rays from heavy-ion collisions

B. A. Remington and M. Blann
Lawrence Livermore National Laboratory, University of California, Livermore, California 94550

G. F. Bertsch
National Superconducting Cyclotron Laboratory and Department of Physics, Michigan State University, East Lansing, Michigan 48824

(Received 20 January 1987)

A model based upon nucleon-nucleon (n-p) bremsstrahlung is presented as a possible explanation of high energy γ rays produced in heavy-ion collisions. A semiclassical bremsstrahlung formula is "calibrated" to p + d bremsstrahlung data, then incorporated into the Boltzmann master equation as a means for following the nucleon-nucleon collisions. The input parameters to the master equation are taken from previous studies of preequilibrium nucleon spectra, eliminating all free parameters from our calculation. The results of this calculation are compared to the available high energy γ-ray data, with generally excellent agreement. Data taken with lead glass detectors are generally underestimated in our model calculation.

I. INTRODUCTION

Results of several experimental programs of measurement of high energy γ rays in heavy-ion induced reactions have been reported quite recently.[1-8] The γ rays observed have energies far in excess of the energy per nucleon of the projectile. How the γ rays achieve these high energies (e.g., in excess of 100 MeV) is a challenging question; there is hope that in answering this question the data will become a probe of the early time history of the reactions, relatively free from reabsorption effects which complicate the interpretation of measurements of subthreshold pions.

For theoretical interpretation of existing data, attempts have been made at descriptions utilizing thermal-statistical emission from a "fireball,"[9,10] cooperative collision effects utilizing virtual clusters,[11] nucleus-nucleus bremsstrahlung,[9,12,13] nucleon-nucleus bremsstrahlung,[14,15] and utilizing nucleon-nucleon bremsstrahlung.[15-19] The calculations using nucleon-nucleon bremsstrahlung either are based upon an assumption of emission in the first collision[15-17] or rely on a model to follow the nucleon-nucleon collisions throughout the relaxation process.[18,19] The latter approach to date has been used either with the Boltzmann-Uehling-Uhlenbeck (BUU) model[18] to follow the collisions both in configuration and in momentum space, or with the Boltzmann master equation (BME) approach[19] to follow the collisions in energy space. The former has the advantage of direct access to the gamma-ray angular distribution, while the latter utilizes only a fraction of the computation time and still gives good predictions of the γ-ray energy spectra.

In the present work we investigate the possibility that the γ rays in question result from (incoherent) neutron-proton collisions in the interacting nuclei via a n-p bremsstrahlung (dipole) radiation process. Multiple collision contributions are included in the calculation. The approach taken will be to use the Boltzmann master equation[20-24] to follow the time dependent intranuclear nucleon-nucleon (N-N) collision process of the heavy-ion reaction. If the BME calculations reproduce this nucleon cascade process satisfactorily, we need only to evaluate the n-p bremsstrahlung differential cross section in order to calculate the spectral yields. Indeed, the BME has been very successful in reproducing the high energy neutron spectra from central heavy-ion collisions similar to some of those to be considered in this work.[22,23] This supports the validity of the nucleon distribution we calculate during the intranuclear cascade of the relaxation process. Addition of experimental $N + N \rightarrow N + N + \pi^0$ excitation functions to this calculation yielded excellent agreement with experimental heavy-ion subthreshold pion production cross sections,[24] peaking interest in the viability of using the same code and parameters to address the question of the high energy γ rays.

In Sec. II we briefly review the BME formulation and the changes necessary for the calculation of γ-ray spectra. In Sec. III we discuss the very important question of the differential cross section $(d^2\sigma/dE_\gamma d\Omega_\gamma)$ for the production of γ rays when a np pair of energy i and j collide. We discuss several approaches and make comparisons with available data, indicating finally the formulation which we will use with the BME. We additionally will describe the details of the averaging procedures applied to the radiation formula adopted before its insertion into the BME. In Sec. IV we show results of our calculations versus those published experimental results of which we were aware at the time of this work, and discuss those comparisons. We then show the relationship of the predicted γ-ray spectra to reaction timescales, as this relates to the possibility that these measurements will aid in understanding the early reaction time history. Our conclusions constitute Sec. V.

II. DESCRIPTION OF THE EQUILIBRATION MODEL

A. The Boltzmann master equation (BME)

The Boltzmann master equation model stems from the work of Harp, Miller, and Berne[25,26] as generalized by Blann[20–22] for use in heavy-ion collisions. At the core of the model are three sets (corresponding to nn, pp, and np scattering) of coupled differential equations that define a Boltzmann-like equation for describing the time rate of change of nucleons or holes occupying a given energy level in the nuclear well. These equations can be written as

$$\frac{dN_i^x}{dt}=g_i^x\sum_y\left\{\sum_{jkl}{}'[\omega^{xy}_{kl\to ij}g_k^x g_l^y g_j^y n_k^x n_l^y(1-n_i^x)(1-n_j^y)-\omega^{xy}_{ij\to kl}g_j^y g_k^x g_l^y n_i^x n_j^y(1-n_k^x)(1-n_l^y)]-n_i^x\omega^x_{i\to i'}\right\}+f_i(\mathrm{p,n})\ , \tag{1}$$

the prime on the summation sign indicating that the summations are conducted respecting energy conservation. The superscripts x,y differentiate neutrons from protons in a two-component Fermi gas, and the subscript i denotes the energy of a 1-MeV-wide bin above the bottom of the nuclear well. The g_i^x give the density of single-particle states at energy i for nucleons of type x, as calculated in the Fermi gas model. The n_i^x denote the fraction of levels in the 1-MeV-wide bin at energy i which are occupied by a nucleon of type x, and the Pauli exclusion principle is embodied in the $1-n_i^x$ factors. The $\omega^{xy}_{kl\to ij}$ represent the rate at which a nucleon of type x at energy k scatters from a nucleon of type y at energy l to give nucleons at energies i and j:

$$\omega^{xy}_{kl\to ij}=\frac{\sigma_{kl}[(2/m)(\epsilon_k+\epsilon_l)]^{1/2}}{V\sum_{q,p}{}'g_q g_p} \tag{2}$$

where V is the nuclear volume and σ_{kl} is the free nucleon-nucleon scattering cross section for nucleons of energy $k+l$ as computed from the equations of Chen *et al.*[27] The $\omega^x_{i\to i'}$ in Eq. (1) give the rate of transmission of an x-type nucleon at energy i into the continuum at energy i'. These rates are calculated from the rate of capture of nucleon x at laboratory energy i' into the nucleus at energy i, making use of the reciprocity theorem. The last term, $f_i(\mathrm{p,n})$, is the injection term, which gives the rate of insertion into the nuclear well of nucleons at energy i from the projectile nucleus. A constant velocity of approach is assumed based upon the nucleus-nucleus center-of-mass energy above the Coulomb barrier. The density of the fusing system is also assumed to remain constant.

B. Dynamics of the fusion process

The BME is a straightforward semiclassical technique with which to follow the relaxation process of excited nucleons in a Fermi gas nucleus. The difficult question in applying the model to heavy-ion reactions is that of the time dependent injection of nucleons in the fusion-coalescence process. How does the Fermi motion couple with the beam velocity to distribute the excited nucleons in the energy space of our model?

The approach which has been taken to answer this question is largely based on earlier work for light-ion precompound decay processes, e.g., alpha particle induced reactions. We make some assumptions about the distribution of nucleon energies, perform the evaluation of the BME using these assumptions, and then see if we have broad success in reproducing a large body of data as an *a posteriori* justification of the original assumptions.

Two main assumptions made are (1) that the lighter partner in the heavy-ion reaction is considered to be the projectile, with mass number A_p, and (2) the projectile nucleons randomly couple their Fermi and beam velocities such that any partition of energies between A_p nucleons (which we refer to as n_0 excitons) occurs with equal *a priori* probability. We further assume that the energy which is partitioned is the excitation energy that would be available if a compound nucleus were formed, i.e., the center of mass energy plus the Q value for fusion. This distribution is given by an expression due to Ericson[28] for the partition of energy E between $n_0=A_p$ excitons consisting of p particles and h holes (we assume $\mathrm{p}=A_p$, $\mathrm{h}=0$) with a constant single particle level density "g" as

$$N(E)dE=\frac{(gE)^{n-1}}{\mathrm{p!h!}(n-1)!}\ . \tag{3}$$

One might wish to impose an additional constraint on the distribution. The Ericson expression permits a single nucleon to have the entire excitation energy, albeit with an extremely low probability. However, in the semiclassical limit that the Fermi momentum distribution at zero temperature has a sharp upperbound at the Fermi energy, there is a limit $\epsilon_{\max}$ to the energy which a single nucleon may have (before rescattering). This limit is given by

$$\epsilon_{\max}=(\sqrt{\epsilon_F}+\sqrt{\epsilon_{\mathrm{beam}}})^2\ , \tag{4}$$

where ϵ_F is the Fermi energy and ϵ_{beam} is the beam energy in MeV/nucleon. We will generally use Eq. (3) modified for the constraint of Eq. (4), which we will call the sharp-cutoff distribution. In a few cases, however, we will show results of using Eq. (3) unmodified, which we will refer to as the Ericson distribution. This will let us test the upper limit of effects due to high momentum components in a quantal system.

Earlier works using Eq. (3) gave excellent agreement with experimental neutron spectra from 10, 15, and 20 MeV/nucleon ^{20}Ne and 25 MeV/nucleon ^{12}C projectiles on Ho targets.[22,23] The experiments were gated on central collisions, which is the case we assume in our model calculations. The agreement with these data support the conclusion that Eq. (3) gives a reasonable representation

of the initial excited nucleon distribution. We now wish to calculate the γ-ray spectra resulting from the intranuclear collisions of these nucleons. We describe modifications to the BME for calculating the high energy γ-ray spectra in the next section.

III. BME MODIFICATIONS FOR HIGH ENERGY γ-RAY CALCULATIONS

A. Code modification

The extension of Eq. (1) to include N-N bremsstrahlung processes, is, in principle, straightforward. We need only include a term giving the inelastic cross section per unit time between nucleons of energy i and j to give a photon of energy ϵ_γ. Hence we write

$$\frac{d^2\sigma}{dE_\gamma dt} = \sum_{ijkl}{}' \omega_{ij\to klm}^{\mathrm{pn}\gamma} g_i^{\mathrm{p}} g_j^{\mathrm{n}} g_k^{\mathrm{p}} g_l^{\mathrm{n}} n_i^{\mathrm{p}} n_j^{\mathrm{n}} (1-n_k^{\mathrm{p}})(1-n_l^{\mathrm{n}}) \sigma_R \ , \tag{5}$$

where σ_R is the reaction cross section for a central collision, approximated as $\sigma_R = \pi r_0^2 A^{2/3}$, with $r_0 = 1.2$ fm. Such an additional term needs only to be summed over time, just as is done to get the nucleon spectra. What is needed is a theoretical equation which will give the free npγ double differential inelastic cross section for any value of the initial nucleon pair energies and for any value of the γ-ray energy. This would define the $\omega_{ij\to klm}$ of Eq. (5), and the γ-ray spectra would immediately follow. Before adopting a theoretical expression for calculating γ-ray yields in heavy-ion reactions, we would first wish to compare its predictions with free npγ data. It is essential to confirm that the theoretical results upon which our model calculations are based are, in fact, in good agreement with a large body of experimental data. Unfortunately, these tasks are difficult and ambiguous. There is by no means agreement on the "correct" theoretical formulation, and the data set available for comparison is sparse, with large uncertainties. We will first discuss the question of theoretical formulations for the inelastic spectra, followed by a discussion of and comparison with experimental results. From this we will select the theoretical expression to be used, with no further adjustment, to calculate the γ-ray emission in heavy-ion reactions.

B. Theoretical bremsstrahlung calculation

The nn and pp bremsstrahlung cross sections have been shown to be small compared to the npγ cross sections.[29–34] We therefore consider only the latter case. Our starting point is a semiclassical result with two quantal corrections added,[15,19,35]

$$\frac{d^2N}{dE_\gamma d\Omega_\gamma} = \frac{1}{E_\gamma}\frac{\alpha}{(2\pi)^2}\sum_{k=1}^{2}\left|\frac{\hat{\epsilon}_k\cdot\boldsymbol{\beta}_i}{1-\hat{\mathbf{q}}\cdot\boldsymbol{\beta}_i}-\frac{\hat{\epsilon}_k\cdot\boldsymbol{\beta}_f}{1-\hat{\mathbf{q}}\cdot\boldsymbol{\beta}_f}\right|^2 \mathrm{P}_{\mathrm{fac}}(1+X) \ . \tag{6}$$

Here, $\alpha = \frac{1}{137}$ is the fine structure constant, β_i and β_f are the proton initial and final velocities and, $\hat{\epsilon}_1$, $\hat{\epsilon}_2$, and $\hat{\mathbf{q}}$ are unit vectors designating the two directions of polarization and the direction of propagation of the γ ray. The last two factors are quantal corrections to the semiclassical result. The P_{fac} is a correction due to final state phase space,[15] and the assumed form is $P_{\mathrm{fac}} = (\beta_f\gamma_f)/(\beta_i\gamma_i)$, where γ is the relativistic contraction factor. Integrating Eq. (6) over solid angle yields the multiplicative factor necessary to convert the $\omega_{ij\to kl}$ of Eq. (2) to the $\omega_{ij\to klm}$ of Eq. (5). Brown and Franklin did more rigorous quantal calculations[34] of the N-N bremsstrahlung process, and concluded that meson exchange effects caused approximately a factor of 2 increase in the γ-ray production cross sections versus the results of Eq. (6). We therefore have added the factor $1+X$ to Eq. (6), where $X=0$ gives the semiclassical result modified only for the phase space factors, and where $X=1$ represents crudely a correction for the meson exchange effects. We emphasize that Brown and Franklin did a full quantal calculation including meson exchange effects; unfortunately, the results of Ref. 34 are not in a form which is convenient for use in the master equation.

We note a recent and very interesting result of Neuhauser and Koonin.[10] They have generalized the quantum mechanical bremsstrahlung calculation of Brown and Franklin[34] to produce angle-integrated γ-ray spectra. They point out that for high energy γ rays approaching the kinematic limit, the neutron and proton in the exit channel are moving at very low relative velocity. Hence, the overlap of their wave functions in the exit channel is very large, resulting in a much larger bremsstrahlung cross section than the classical result would predict. The work of these authors predicts that the corrections to Eq. (6) due to quantal effects are not constant (as we have assumed), but rather are a function of final nucleon energy. These authors disagree with the necessity of the phase space factor in Eq. (6). We will consider the results of Neuhauser and Koonin, as well as results of Eq. (6) in comparisons with npγ data, and with a few sets of heavy-ion γ-ray data.

C. Comparison of experimental and theoretical npγ data

Ideally, we would like to have a large body of npγ-ray differential cross sections with which to compare the calculations described in the preceding subsection. To our knowledge, there have been only a few measurements of this type.

In Table I we compare yields calculated with Eq. (6) with $X=0$ with the data of Brady and Young[36] for a 208 MeV neutron beam and of Edgington *et al.*[37] for a 130 MeV neutron beam, both incident on a liquid hydrogen target. Here the form of the data does not offer an unambiguous comparison. The experimental results are expressed as $d^2\sigma/d\Omega_{\mathrm{p}}d\Omega_{\mathrm{n}}$, i.e., as the double differential cross section for detecting the scattered neutron and proton at angles kinematically removed from the elastic region. To allow a comparison with our bremsstrahlung

TABLE I. Comparisons of calculated and experimental pnγ cross sections. Data are for 208 MeV (Ref. 36) and 130 MeV (Ref. 37) neutron beams on liquid hydrogen targets. Details of the intercomparisons between experimental and calculated results are discussed in the text.

Ref.	(θ_n,θ_p) (deg)	$\frac{d^2\sigma}{d\Omega_n d\Omega_p}$ (μb/sr^2)	Calc. (μb/sr^2)	Expt./ Calc.
36	30,30	35±14	14	2.5
36	35,35	57±13	38	1.5
36	38,38	116±20	96	1.2
36	40,30	114±44	48	2.4
36	45,30	132±53	105	1.3
37	23,20	47±35	8	5.9
37	26,20	16±29	10	1.6
37	29,20	35±28	13	2.7
37	38,20	64±24	26	2.5
37	23,32	17±29	8	2.1
37	26,32	66±29	11	6.0
37	29,32	77±32	15	5.1
37	38,32	116±21	44	2.6

formula, we write the following:

$$\frac{d^2\sigma}{d\Omega_p d\Omega_n}\Delta\Omega_p\Delta\Omega_n=\int \frac{d^2N}{dE_\gamma d\Omega_\gamma}d\Omega_\gamma\frac{d\sigma}{d\Omega_p}\Delta\Omega_p\Delta E_\gamma \ , \quad (7)$$

where $\Delta\Omega_p$ and $\Delta\Omega_n$ are the solid angles subtended by the proton and neutron detectors, respectively. The ΔE_γ is the spread in the kinematically allowed γ-ray energies that results from the finite solid angle of the neutron detector ($\Delta\Omega_n$), and $d\sigma/d\Omega_p$ is the differential p-n elastic scattering cross section. To calculate the ratio $\Delta E_\gamma/\Delta\Omega_n$, we consructed a five-dimensional transformation array of derivatives relating the directions of the proton, neutron, and γ ray and the energy of the γ ray. The Jacobian, as calculated by taking the determinant of this array, then yields the desired ratio. For a few test cases, we checked these results with a Monte Carlo calculation which incorporated the actual experimental acceptances of Refs. 36 and 37. The results from the two methods were consistent with one another. Using the ratios as calculated by the Jacobian method, Eq. (7) is then solved for $d^2\sigma/d\Omega_p d\Omega_n$ and compared with the experimental data. The result of Eq. 6 ($X=0$) is about a factor of 1.8 lower than the data of Brady and Young,[36] and about a factor of 3.6 lower than the data of Edgington *et al.*[37] We qualify this comparison by pointing out the very large error bars (counting statistics) of the experimental data and the additional uncertainty of the beam energy [$\Delta E_{\rm FWHM}/E\sim 0.22$ (FWHM denotes full width at half maximum)].

We present some additional comparisons of Eq. (6) with integrated results deduced from experiments in Table II. The first two integrated cross sections in Table II are the results deduced by Edgington and Rose[29] for "free" nucleon-nucleon scattering. The predictions of Eq. (6) with $X=0$ are about a factor of 3.5 too low. To arrive at the pnγ estimate in Table II, Edgington and Rose start with their p + Be data and then introduce a scaling factor

TABLE II. Comparison of cross sections calculated with the semiclassical bremsstrahlung formula of Eq. (6) with the "free" pnγ bremsstrahlung data of Ref. 29 (140 MeV proton beam on a liquid hydrogen target) and Ref. 30 (197 MeV proton beam on a liquid deuterium target).

Ref.	Energy range of γ ray	Expt. $\sigma_{\rm tot}$ (μb)	Calc. $\sigma_{\rm tot}$ (μb)	Expt./ Calc.
29	$E_\gamma>30$ MeV	14	4.1	3.4
29	$E_\gamma>40$ MeV	8	2.2	3.6
30	$E_\gamma>40$ MeV	35±12	7.4	4.7

of 2 based upon a calculation from another work to take into account the Pauli exclusion principle. We also present the integrated result of Kohler *et al.*[30] for a 197 MeV proton beam on a liquid deuterium target. Our prediction is a factor of 4.7 lower than this result, but Kohler *et al.* note that their result is inconsistent with that of Edgington and Rose,[29] with the discrepancy never having been resolved.[38] The combination of integrating over energy, introducing an additional scaling, and the disagreement between the results of Refs. 29 and 30 make it difficult to assess the physical significance of these comparisons with our calculation.

A data set more closely related to our need of a γ-ray spectrum versus N-N energy comes from the 140 MeV p + d measurement by Edgington and Rose.[29] Because the p-p bremsstrahlung cross section is very much smaller than the p-n bremsstrahlung cross section,[29–34] the p + d result should be a good approximation to the p + n value, especially if we make a correction for the neutron momentum distribution in deuterium. We therefore compare the spectra predicted by Eq. (6) with the data of Ref. 29, effectively "calibrating" Eq. (6) before applying it to all nucleon energies for the heavy-ion reactions to be considered. This places a very heavy dependence on the assumed correctness of this one data set. It is very important for the future to have this measurement repeated using higher resolution detectors, and for different proton energies.

A sample of these comparisons is shown at the top of Fig. 1. The short-dashed curve corresponds to Eq. (6) with $X=0$ (no estimated correction for meson exchange) for free p-n bremsstrahlung, viz., the yield from Eq. (6) was averaged over final proton direction and integrated over final γ-ray direction. The result is seen to be too low compared to the data. The long-dashed curve is the same formula applied to p-n bremsstrahlung, but with the momentum of the neutron in deuterium distributed according to the calculation of Ciofi degli Atti *et al.*[39] Folding in the momentum distribution of the neutron in deuterium increases the bremsstrahlung yield somewhat, but the calculated result still underpredicts the data by about a factor of 2. The solid line in Fig. 1 corresponds to a calculation similar to that of the long-dashed curve, except with $X=1$ in Eq. (6), consistent with the method used in Ref. 19. This calculation reproduces the experimental spectrum quite well. Therefore, this is the fundamental pnγ bremsstrahlung cross section that we will adopt for

use throughout this work. This may be justified most easily on an *ad hoc* basis; it gives good agreement with the (p,d) result. We have also folded the Neuhauser-Koonin result[10] into our deuteron calculation, and the result is shown as the dotted-dashed line in Fig. 1. Their quantum-mechanical result seems to significantly overpredict the experimental spectrum.

Having selected a "calibrated" expression for the pnγ cross section, we next apply the master equation to p-nucleus and heavy-ion—nucleus data. The BME parameters are precisely those used earlier for calculating preequilibrium neutron spectra.[22,23] The BME code follows the nucleon-nucleon collisions in the relaxation process only in energy space. Therefore, suitable averaging has to be applied to Eq. (6) before the pnγ cross sections can be inserted into the master equation. In particular, the BME assumes a perpendicular initial collision configuration delimited only by the total nucleon kinetic energy ($\epsilon_{\rm tot}=i+j$). For each $\epsilon_{\rm tot}$, then, the cross section from Eq. (6) is averaged over all initial collision configurations and over all final nucleon directions. We neglect the momentum carried by the γ ray and it is assumed to be emitted at 90°. The effect of each of these approximations on the calculated cross sections is estimated to be less than about 20%. In addition, the BME code folds in the nucleon-nucleon scattering cross section, again assuming a perpendicular collision configuration. To correct for this approximation, we have multiplied Eq. (6) by the ratio of the correctly averaged pn scattering cross section to that assumed by the BME. Except where otherwise noted, we have set $X=1$ in Eq. (6), which is consistent with the findings of Brown and Franklin[34] that inclusion of meson exchange currents results in about a factor of 2 increase in the bremsstrahlung cross sections.

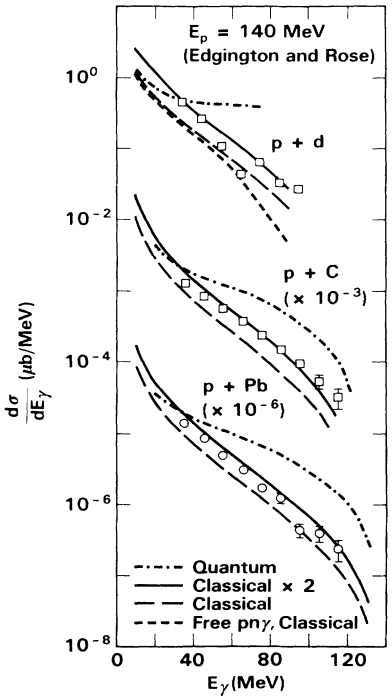

FIG. 1. Comparisons of calculations with high energy γ-ray data of Ref. 29 for a 140 MeV proton beam. At the top, the p + d data are used as a standard with which to "calibrate" our pnγ bremsstrahlung equation. The short-dashed line corresponds to a semiclassical bremsstrahlung formula for free nucleon-nucleon scattering. The long-dashed line is the same, only with the momentum distribution of the target neutron in deuterium taken into account. The solid line corresponds to the deuteron calculation multiplied by 2 to crudely account for the effect of meson exchange. The dotted-dashed line corresponds to folding the quantum bremsstrahlung result of Ref. 10 into the deuteron calculation. The lower two spectra show γ-ray data for p+^{12}C and p + Pb. The curves represent calculations with the master equation using the semiclassical bremsstrahlung cross sections (dashed lines), the semiclassical cross sections multiplied by 2 for meson exchange (solid lines), and the quantum bremsstrahlung cross sections (dotted-dashed lines).

IV. RESULTS OF NUCLEON-NUCLEUS AND NUCLEUS-NUCLEUS DATA VERSUS MODEL COMPARISONS

A. p-nucleus results

Comparisons of the BME predictions using Eq. (6) are shown versus the 140 MeV p+^{12}C and p + Pb data[29] in Fig. 1. We show results both for $X=0$ and 1. It may be seen that, as for the p + d case, the $X=1$ choice gives excellent agreement with the experimental results. For p-nucleus reactions, we do not assume an initial distribution of proton energies as given, e.g., by Eq. (3); the proton enters the potential at a discrete energy and commences the cascade which is followed by the BME. These comparisons therefore test Eq. (6) with interactions with target nucleons having a Fermi momentum distribution without additional assumptions on entrance channel momentum coupling. Aside from a single projectile nucleon (having a discrete incident energy), all other parameters of the BME are those used to successfully reproduce preequilibrium neutron and subthreshold pion production.[22–24]

We also show results using the pnγ cross sections of Neuhauser and Koonin[10] in the BME for p+^{12}C and p + Pb in Fig. 1. As for the p + d case, there is a pronounced overprediction of the data.

B. Nucleus-nucleus results

Figure 2 shows the γ-ray spectra reported by Stevenson *et al.*[2] for a ^{14}N beam on targets of ^{12}C and Pb at 20, 30, and 40 MeV/nucleon. As discussed in Sec. II, we assume a sharp-cutoff initial exciton distribution. Since the master equation follows the intranuclear cascade only in energy space, we do not have ready access to the γ-ray angular distribution. Therefore, to compare our results to the $d^2\sigma/dE_\gamma d\Omega_\gamma$ data of Ref. 2, we note that at $\theta_{\rm lab}=90°$ the lab and center-of-mass spectra are the same to within a factor of $\gamma_{\rm c.m.}\sim 1$, the relativistic contraction factor of the center of mass. We further assume that the angular distribution is nearly isotropic in the nucleus-nucleus center-of-mass system. Therefore, by dividing the predicted center-of-mass $d\sigma/dE_\gamma$ by 4π, we obtain a prediction for $d^2\sigma/dE_\gamma d\Omega_\gamma$ at $\theta_{\rm lab}=90°$. Inspection of the angular dis-

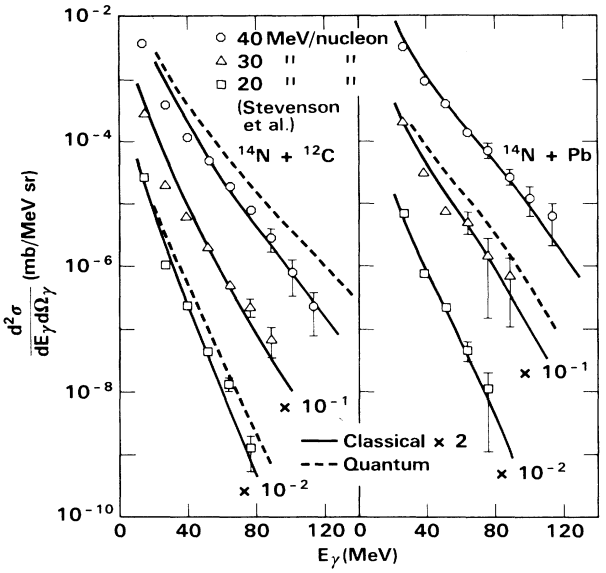

FIG. 2. The γ-ray data of Ref. 2 are shown for ^{14}N+^{12}C and for ^{14}N+Pb at 20, 30, and 40 MeV/nucleon. The solid lines correspond to the master equation calculation using the "calibrated" semiclassical bremsstrahlung cross sections, while the dashed lines correspond to quantum bremsstrahlung cross sections.

tribution presented in Ref. 2 shows that our approximation of isotropy in the c.m. system introduces less than about 20% uncertainty in our calculated spectra. The main difference between this figure and Fig. 1 of Ref. 19 is the slight refinement in our calculation mentioned above to overcome the approximation in nucleon scattering cross sections made in the BME code, which assumes perpendicular collision geometry. The net effect is to lower our result by about 20%, which does not alter our previously reported agreement with the data. We also display in Fig. 2 the results from using the quantum bremsstrahlung cross sections of Neuhauser and Koonin[10] at two energies for the ^{12}C target and at one energy for the Pb target. As in Fig. 1, this result somewhat overpredicts the experimental spectra, though the discrepancy is not so striking for the heavy-ion collisions as for the p-nucleus data.

In Fig. 3 we display the results of Njock *et al.*[3] for ^{40}Ar+^{197}Au at 30 MeV/nucleon at $\theta_{lab}=90°$. The calculated center-of-mass $d\sigma/dE_\gamma$ was transformed to $d^2\sigma/dE_\gamma d\Omega_\gamma$ in the same manner as for Fig. 2. Setting $n_0=A_{proj}$ for the initial exciton distribution function has not yet been tested on preequilibrium nucleon spectra for projectile nuclei as heavy as ^{40}Ar. Hence, this extrapolation is presently without independent support from gated coincidence spectra as to its ability to reproduce the nucleon emission spectra and, therefore, by implication, the internal nucleon distribution. A recent singles nucleon emission measurement for ^{40}Ar induced reactions does support the assumption that $n_0=A_p=40$;[40] we would, however, prefer to rely upon evaporation residue gated results. The agreement of the calculated spectrum in Fig. 3 with the data is striking, in view of the caveat with respect to the initial exciton distribution function.

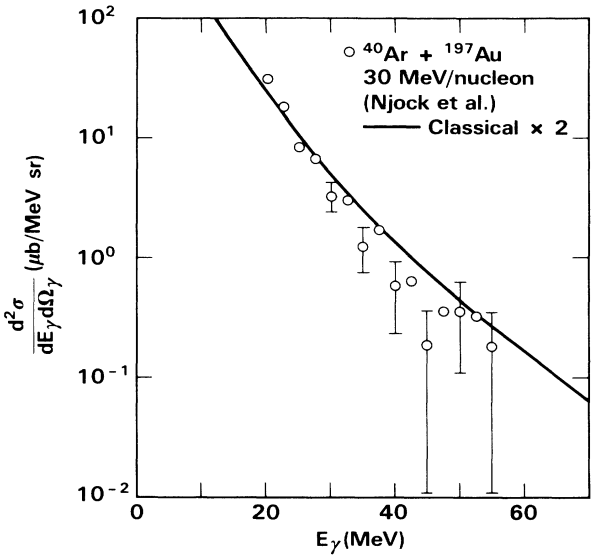

FIG. 3. The γ-ray data of Ref. 3 for ^{40}Ar+^{197}Au at 30 MeV/nucleon. The solid line represents the master equation calculation using the "calibrated" semiclassical bremsstrahlung formula.

Figure 4 shows experimental spectra for a 44 MeV/nucleon ^{86}Kr projectile on targets of ^{12}C (Ref. 4) and on ^{nat}Ag (Ref. 5). The upper spectrum corresponds to $\theta_{lab}=90°$ and the lower spectrum to $\theta_{lab}=100°$. For both cases, the calculation assumes $\theta_{lab}=90°$ and the transformation to double-differential spectra was handled as discussed above. For the ^{86}Kr+^{12}C system, we assume $n_0=12$ for the initial exciton number, whereas for the

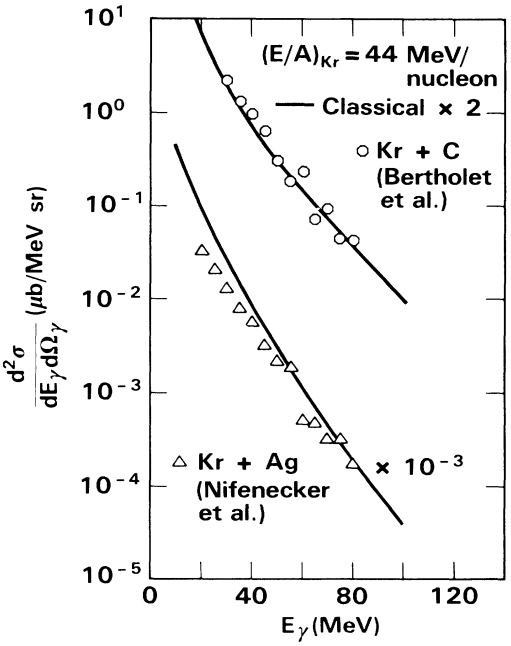

FIG. 4. Same as for Fig. 3 for the data of Ref. 4 for ^{86}Kr+^{12}C (upper) and of Ref. 5 for ^{86}Kr+^{nat}Ag (lower), both at 44 MeV/nucleon.

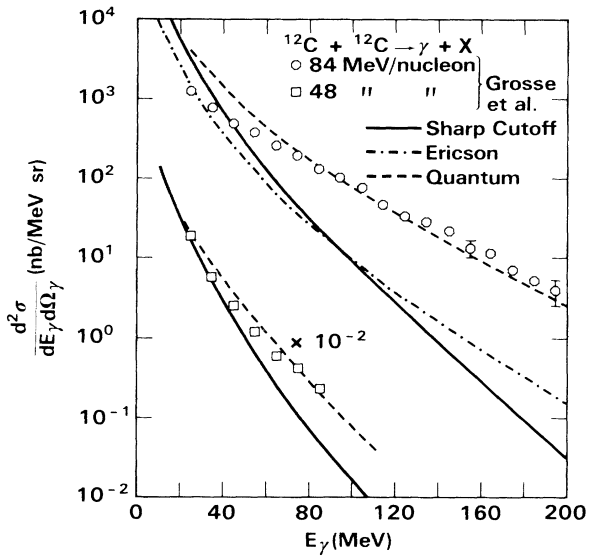

FIG. 5. γ-ray data (Ref. 7) for $^{12}C+^{12}C$ at 84 MeV/nucleon (upper) and 48 MeV/nucleon (lower). The solid lines represent the master equation calculation for a sharp-cutoff initial exciton distribution, while the dotted-dashed line is for an Ericson exciton distribution. The dashed lines represent master equation calculations using the quantum bremsstrahlung cross sections.

$^{86}Kr+^{nat}Ag$ system we use $n_0=A_{proj}=86$. Again, we point out that this assumption is unsupported for $A_{proj}>20$. For both spectra presented in Fig. 4, the agreement between experiment and calculation is excellent.

In Fig. 5 we present comparisons with the results of Grosse *et al.*[6,7] for $^{12}C+^{12}C$ at 48 and 84 MeV/nucleon. The experimental spectra are for 90° in the center-of-mass frame. Again, we simply divide the calculated center-of-mass differential energy spectra by 4π to compare with the experimental results. Examination of the angular distribution presented in Ref. 6 shows that this introduces probably less than 20% error. The experimental yield has been reduced by 36% from the published results to account for a detector recalibration.[41] The solid lines correspond to a sharp-cutoff initial exciton distribution, as used in Figs. 1–4, and this result falls significantly below the experimental data. We show (for 84 MeV/nucleon) the results of replacing the sharp cutoff initial exciton spectrum by an Ericson distribution. This gives an estimate of whether or not the discrepancy might be understood in terms of high momentum components in the Fermi momentum distribution. This brings the slope closer to that of the data, but the absolute magnitude of the calculation is still about an order of magnitude too low. (Using the Ericson distribution for the 48 MeV/nucleon data does not change the predicted spectrum appreciably.) We point out by way of the dashed lines that folding the Neuhauser-Koonin quantum bremsstrahlung cross section into the master equation [instead of using Eq. (6)] for this data set gives good agreement with the experimental result.

In Fig. 6 we show calculations (using the sharp-cutoff initial exciton distribution) compared to the Grosse *et al.* data for $^{12}C+^{238}U$ at 84 MeV/nucleon (Ref. 6) (top) and for $^{12}C+^{12}C$ at 74 MeV/nucleon (middle) and 60 MeV/nucleon (Ref. 7) (bottom). The results are similar to those of Fig. 5, in that we significantly underpredict the data, both for a ^{12}C target and a ^{238}U target.

In Fig. 7 we show the results of Alamanos *et al.*[8] for $^{14}N+Ni$ at 35 MeV/nucleon. Since the angular distribution presented in their work shows a non-negligible anisotropy, their results displayed here have been averaged over angle. Our prediction has been prepared in the same manner as discussed above, and our calculated result falls significantly lower than the experimental data. At this beam energy, using the Ericson distribution would only make a small change, as shown in our earlier work.[16]

V. DISCUSSION

The comparisons in Figs. 1–7 show excellent results in Figs. 1–4 and underprediction in Figs. 5–7. If the pnγ interpretation is correct (an open point), then there are two possibilities to consider; inconsistencies in the data sets, or a change in reaction mechanism at the higher beam velocities. The most crucial issue concerning the former is that of a detector calibration, which we discuss next. A necessary condition for the latter is a smooth and systematic divergence in the cross section from a dominant incoherent pnγ mechanism as a function of beam

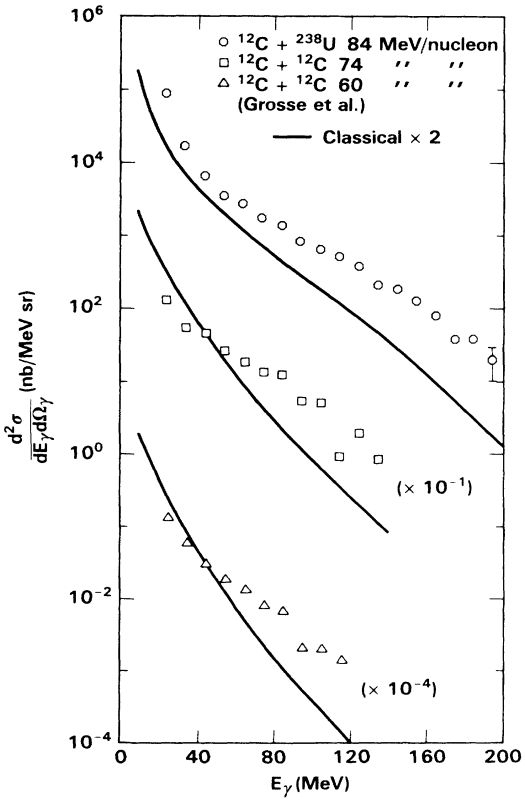

FIG. 6. Same as for Fig. 3 (data of Refs. 6 and 7) for $^{12}C+^{238}U$ at 84 MeV/nucleon (top), and $^{12}C+^{12}C$ at 74 MeV/nucleon (center) and 60 MeV/nucleon (bottom).

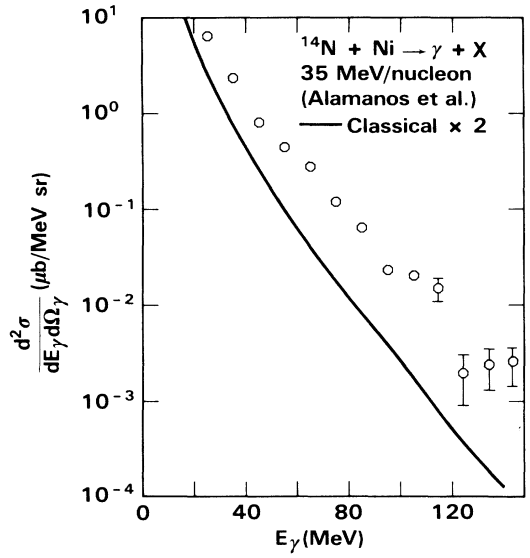

FIG. 7. Same as for Fig. 3 (data of Ref. 8) for ^{14}N+Ni at 35 MeV/nucleon.

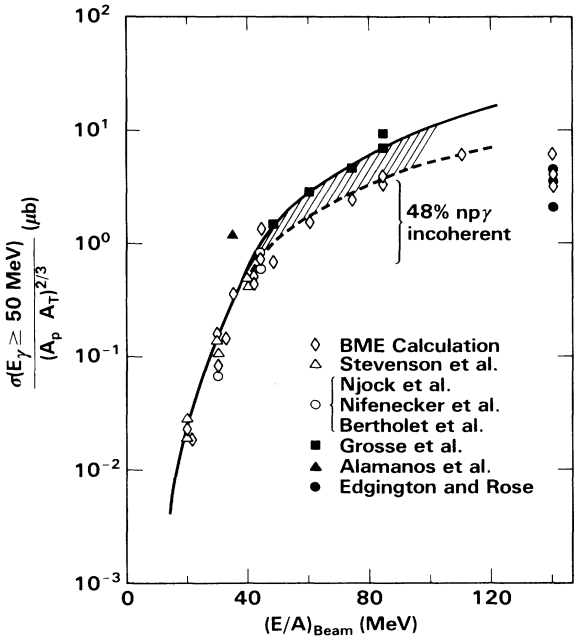

FIG. 8. Display of integrated γ-ray cross sections above 50 MeV scaled by $(A_pA_T)^{2/3}$ for all of the experimental and calculated results discussed in the text. The calculated results are plotted with open diamonds, while the remaining open and solid symbols correspond to the experimental results, as defined in the legend. The solid and dashed curves drawn through the experimental and calculated results, respectively, are meant only to guide the eye. The hatched area illustrates the region where data and calculation start to disagree.

velocity. This point is discussed further below.

The p-nucleus data of Fig. 1, which we used for our "calibration," were taken with a telescope consisting of three plastic scintillators and a lead glass calorimeter. The authors performed painstaking calibrations of their detector, including use of an electron synchrocyclotron. We refer the reader to Ref. 29 for a detailed description of the calibration procedures used by Edgington and Rose. The data shown in Figs. 5—7 were taken with lead glass Čerenkov calorimeter detectors, and the data of Figs. 2—4 were taken with multiple plastic Čerenkov arrays or with combinations of plastic Čerenkov and NaI detectors.[2—8] A description of the combination of modeling, calculation, and experimental measurement used to deduce efficiencies for the detectors used by Grosse *et al.*[6,7] may be found in Ref. 42. A question has recently been raised as to the calibration of the lead glass detector used in Refs. 6 and 7; it has been suggested[42] that these cross sections might be reduced by an additional factor of 2. This would bring our calculation into agreement with the data at 48 MeV/nucleon, but we would still underpredict the revised data at 84 MeV/nucleon. The data of Alamanos *et al.*[8] for 35 MeV/nucleon ^{14}N fall between the 30 and 40 MeV/nucleon ^{14}N results of Stevenson *et al.*[2] in beam energy. Yet the γ-ray yields are significantly higher. This data set would appear to be inconsistent with the data of Stevenson *et al.* The question of which data set is better remains a point of debate, and we cannot answer this question. A thorough experimental intercomparison of the several detector designs used in Refs. 2—8 has not, to our knowledge, been completed at this time. Such an intercomparison is obviously important for further interpretation of these data.

Beyond the possibility that there are errors in calibration of the detector systems, there is the intriguing possibility that the higher energy reactions differ in mechanism from those at lower energy. To see if this might be a viable possibility, we display energy integrated γ-ray yields from Figs. 1—7 in Fig. 8.

To create a universal yield for the various disparate systems, we integrate each γ-ray cross section above $E_\gamma = 50$ MeV, then divide by $(A_pA_T)^{2/3}$, effectively giving yield per unit target cross-sectional area per unit projectile cross-sectional area. One sees that all of the heavy-ion data except those of Ref. 8 fall on a smooth curve. (We note that the data of Ref. 8 were taken with lead glass calorimeter detectors whose energy resolution is inherently poor. If the energy resolution could be unfolded from the data, their quoted cross sections might be reduced somewhat. We refer the reader to the discussion of this point in Ref. 8.) Similarly, our calculations also follow a smooth curve, but lower than the data for $E/A_{\text{beam}} \geq 50$ MeV/nucleon. The hatched area on the figure represents the difference. Assuming that the data are correct, this seems to suggest that the reaction mechanism starts to change at around $E/A_{\text{beam}} = 5$ MeV/nucleon. As previously mentioned, the angular distribution presented in Ref. 6 also supports this hypothesis. In exploring this possibility, we draw upon the work of Nifenecker and Bondorf.[9] In their theoretical analysis of the ^{12}C+^{238}U γ-ray data of Ref. 6, the authors develop a model combining nucleon-nucleon bremsstrahlung utilizing a "fireball" scenario with coherent nucleus-nucleus bremsstrahlung.

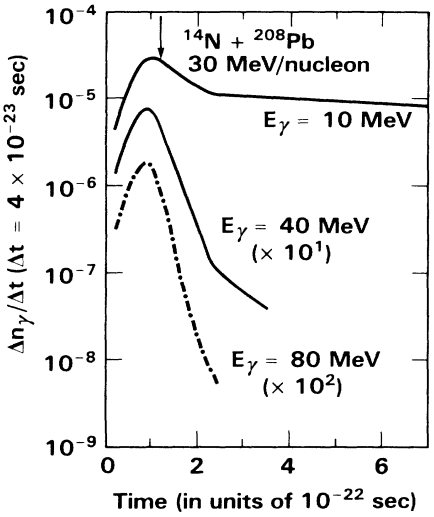

FIG. 9. Number of γ rays emitted as a function of time for γ-ray energies of 10 MeV (top), 40 MeV (middle), and 80 MeV (bottom). The calculation was conducted for $^{14}N+^{208}Pb$ at 30 MeV/nucleon. The arrow at the top of the figure indicates the time for which the colliding nuclei have completely fused.

Their findings indicate that 68% of the γ-ray cross section is due to incoherent pnγ bremsstrahlung, with the remaining 32% due to coherent nucleus-nucleus bremsstrahlung. Our calculated incoherent pnγ cross section for the same system is 50% of the experimental result, consistent (within uncertainties) with the findings of Nifenecker and Bondorf.

In Fig. 9 we present the calculated γ-ray multiplicity as a function of time for γ-ray energies of 10, 40, and 80 MeV for $^{14}N+^{208}Pb$ at 30 MeV/nucleon. One clearly sees that for high energy γ rays the emission occurs very early in the collision process. Indeed, for this system 80 MeV γ rays are emitted within the first 2×10^{-22} s of the reaction, which is slightly less than twice the time necessary for fusion to occur (according to the algorithm used herein). This result implies a first collision origin for the highest energy γ rays within the framework of the pnγ mechanism assumed.

VI. SUMMARY AND CONCLUSIONS

To try to understand the origin of high energy γ rays from intermediate energy heavy-ion collisions, we have adopted a model predicated upon an incoherent pnγ bremsstrahlung mechanism. The essence of the model is that in the preequilibrium nucleon cascade that marks the early moments of the nuclear collision and subsequent relaxation there will be γ rays emitted characteristic of free nucleon-nucleon bremsstrahlung. When the Fermi velocity of a projectile nucleon is coupled to the relative velocity of approach of the projectile nucleus, one can achieve nucleon-nucleon collisions of energy sufficient to emit the observed high energy γ rays through bremsstrahlung. To realistically model this process, we (1) adopted the Boltzmann master equation approach as an established model of the preequilibrium relaxation process, (2) neglected ppγ and nnγ bremsstrahlung processes as being small compared to the pnγ process, and (3) calibrated a semiclassical, incoherent pnγ bremsstrahlung formula to reproduce a reference p + d γ-ray spectrum. The input parameters to the BME code were those established in analyses of prequilibrium neutron spectra[22,23] and further tested in prediction of subthreshold pion production.[24] In this sense our calculations are absolute predictions with no parameters being adjusted to fit the heavy-ion data.

We have been successful in reproducing high energy γ-ray spectra in systems as varied as $p+^{12}C$ and p + Pb at 140 MeV, $^{14}N+^{12}C$ and ^{14}N + Pb at 20, 30, and 40 MeV/nucleon, $^{40}Ar+^{197}Au$ at 30 MeV/nucleon, and $^{86}Kr+^{12}C$ and ^{86}Kr+Ag at 44 MeV/nucleon. We underpredict the data at the highest beam velocities, namely $^{12}C+^{12}C$ and $^{12}C+^{238}U$ at $E/A_{\rm beam}\geq 50$ MeV/nucleon. The systematics of the data and calculations suggests that perhaps $E/A_{\rm beam}=50$ MeV/nucleon represents a threshold above which incoherent pnγ bremsstrahlung is supplemented by coherent nucleus-nucleus bremsstrahlung. An alternative explanation is that there is an inconsistency between data measured with lead glass and plastic Čerenkov or NaI detectors.

Definitive resolution of the origins of these high energy γ rays awaits additional data sets on several fronts: (1) additional heavy-ion γ-ray data sets to help establish unambiguously the systematics with beam energy and nucleus size, (2) additional high quality "free" nucleon-nucleon bremsstrahlung data, to complement earlier results and to confirm a proper basic pnγ formula to be used, e.g., in the BME, and (3) resolution of questions as to the calibrations of the detectors used in the heavy-ion experiments. Additionally, to justify the BME predictions for $A_{\rm proj}>20$, it is desirable to have evaporation residue gated nucleon emission spectra to verify the parametrization of the initial exciton distribution.

ACKNOWLEDGMENTS

It is a pleasure to acknowledge many helpful discussions with Dr. V. Brown, Dr. F. Dietrich, and Dr. J. C. Young. We appreciate fruitful discussions with Prof. W. Greiner, Prof. D. Morrissey, Prof. S. Koonin, and Prof. W. Benenson. We are also indebted to Dr. D. Neuhauser for communication of unpublished results. This work was performed under the auspices of the U. S. Department of Energy by the Lawrence Livermore National Laboratory under Contract No. W-7405-ENG-48.

[1]K. B. Beard *et al.*, Phys. Rev. C **32**, 1111 (1985).
[2]J. Stevenson *et al.*, Phys. Rev. Lett. **57**, 555 (1986).
[3]M. Kwato Njock *et al.*, Phys. Lett. **175B**, 125 (1986).
[4]R. Bertholet *et al.*, J. Phys. (Paris) Colloq. **8**, C4-47 (1986).
[5]H. Nifenecker *et al.*, in Proceedings of the XXIVth International Winter Meeting on Nuclear Physics, Bormio, Italy, 1986 (unpublished).
[6]E. Grosse *et al.*, Europhys. Lett. **2**, 9 (1986).

[7]E. Grosse, talk given at the International Workshop on Gross Properties of Nuclei, Hirschegg, 1985 (unpublished).
[8]N. Alamanos *et al.*, Phys. Lett. **B173**, 392 (1986).
[9]H. Nifenecker and J. P. Bondorf, Nucl. Phys. **A442**, 478 (1985).
[10]D. Neuhauser and S. E. Koonin, Nucl. Phys. **A462**, 163 (1987).
[11]R. Shyam and J. Knoll, Nucl. Phys. **A448**, 322 (1986).
[12]D. Vasak, W. Greiner, B. Müller, T. Stahl, and M. Uhlig, Nucl. Phys. **A428**, 291 (1984).
[13]T. Stahl, M. Uhlig, B. Müller, W. Greiner, and D. Vasak, University of Frankfurt report, 1986.
[14]W. Bauer, W. Cassing, U. Mosel, M. Tohyama, and R. Y. Cusson, Nucl. Phys. **A456**, 159 (1986).
[15]K. Nakayama and G. Bertsch, Phys. Rev. C **34**, 2190 (1986).
[16]Che Ming Ko, G. Bertsch, and J. Aichelin, Phys. Rev. C **31**, 2324 (1985).
[17]W. Cassing, T. Biro, U. Mosel, M. Tohyama, and W. Bauer, Phys. Lett. **181B**, 217 (1986).
[18]W. Bauer, G. F. Bertsch, W. Cassing, and U. Mosel, Phys. Rev. C **34**, 2127 (1986).
[19]B. A. Remington, M. Blann, and G. F. Bertsch, Phys. Rev. Lett. **57**, 2909 (1986).
[20]M. Blann, A. Mignerey, and W. Scobel, Nukleonika **21**, 335 (1976).
[21]M. Blann, Phys. Rev. C **23**, 205 (1981).
[22]M. Blann, Phys. Rev. C **31**, 1245 (1985).
[23]M. Blann, in Proceedings of the Symposium on the Many Facets of Heavy-Ion Fusion Reactions, 1986 (Argonne National Laboratory Report ANL-PHY-86-1, 1986, p. 285).
[24]M. Blann, Phys. Rev. C **32**, 1231 (1985).
[25]G. D. Harp, J. M. Miller, and B. J. Berne, Phys. Rev. **165**, 1166 (1968).
[26]G. D. Harp and J. M. Miller, Phys. Rev. C **3**, 1847 (1971).
[27]K. Chen *et al.*, Phys. Rev. **166**, 949 (1968).
[28]T. E. O. Ericson, Adv. Phys. **9**, 423 (1960).
[29]J. A. Edgington and B. Rose, Nucl. Phys. **89**, 523 (1966).
[30]P. F. M. Koehler, K. W. Rothe, and E. H. Thorndike, Phys. Rev. Lett. **18**, 933 (1967).
[31]K. W. Rothe, P. F. M. Koehler, and E. H. Thorndike, Phys. Rev. **157**, 1247 (1967).
[32]J. Ashkin and R. E. Marshak, Phys. Rev. **76**, 58 (1949); **76**, 989(E) (1949).
[33]V. R. Brown, Phys. Rev. **177**, 1498 (1969).
[34]V. R. Brown and J. Franklin, Phys. Rev. C **8**, 1706 (1973).
[35]J. D. Jackson, *Classical Electrodynamics* (Wiley, New York, 1962), p. 703.
[36]F. P. Brady and J. C. Young, Phys. Rev. C **2**, 1579 (1970).
[37]J. A. Edgington *et al.*, Nucl. Phys. **A218**, 151 (1974).
[38]E. H. Thorndike, private communication.
[39]C. Ciofi degli Atti, E. Pace, and G. Salme, Phys. Lett. **141B**, 14 (1984).
[40]A. Fahli *et al.*, Strasbourg University Report CRN/PN 86-29, 1986; Z. Phys. A **326**, 169 (1987).
[41]E. Grosse, private communication.
[42]C. Michel *et al.*, Nucl. Instrum. Methods A **243**, 395 (1986).